



HAL
open science

Tests for the Use of La₂Mo₂O₉-based Oxides as Multipurpose SOFC Core Materials

Julien Jacquens, D. Farrusseng, Samuel Georges, Jean-Paul Viricelle, Cyril Gaudillère, Gwenaël Corbel, Philippe Lacorre

► **To cite this version:**

Julien Jacquens, D. Farrusseng, Samuel Georges, Jean-Paul Viricelle, Cyril Gaudillère, et al.. Tests for the Use of La₂Mo₂O₉-based Oxides as Multipurpose SOFC Core Materials. Fuel Cells, 2010, 10 (3), pp.433-439. 10.1002/fuce.200900099 . hal-00552358

HAL Id: hal-00552358

<https://hal.science/hal-00552358>

Submitted on 6 Jan 2011

HAL is a multi-disciplinary open access archive for the deposit and dissemination of scientific research documents, whether they are published or not. The documents may come from teaching and research institutions in France or abroad, or from public or private research centers.

L'archive ouverte pluridisciplinaire **HAL**, est destinée au dépôt et à la diffusion de documents scientifiques de niveau recherche, publiés ou non, émanant des établissements d'enseignement et de recherche français ou étrangers, des laboratoires publics ou privés.



Tests for the Use of La₂Mo₂O₉-based Oxides as Multipurpose SOFC Core Materials

Journal:	<i>Fuel Cells</i>
Manuscript ID:	face.200900099.R1
Wiley - Manuscript type:	Original Research Paper
Date Submitted by the Author:	18-Dec-2009
Complete List of Authors:	Jacquens, Julien Farrusseng, David Georges, Samuel Viricelle, Jean-Paul Gaudillère, Cyril Corbel, Gwenaël Lacorre, Philippe; Laboratoire des Oxydes et Fluorures, Université du Maine
Keywords:	Oxidation Catalysis, Solid Oxide Fuel Cell, LAMOX, Mixed Ionic Electronic Conduction, Propane, Reduction, Single or Dual Chamber, Stability



Tests for the Use of $\text{La}_2\text{Mo}_2\text{O}_9$ -based Oxides as Multipurpose SOFC Core Materials

J. Jacquens¹, D. Farrusseng², S. Georges³, J.-P. Viricelle⁴, C. Gaudillère^{2,5}, G. Corbel¹, and P. Lacorre^{1,*}

¹Laboratoire des Oxydes et Fluorures, UMR CNRS 6010, Université du Maine, Avenue Olivier Messiaen, 72085 Le Mans cedex 9, France

²IRCELYON, Institut de Recherches sur la Catalyse et l'Environnement de Lyon, UMR CNRS 5256, Université Lyon 1, CNRS, 2 avenue Albert Einstein, 69626 Villeurbanne, France

³Laboratoire d'Electrochimie et de Physico-chimie des Matériaux et des Interfaces, UMR CNRS 5631-INPG-UJF, BP 75, 38402 Saint Martin d'Hères cedex, France

⁴Ecole Nationale Supérieure des Mines, LPMG-UMR CNRS 5148, Département Microsystèmes Instrumentation et Capteurs Chimiques, Centre SPIN, 158 Cours Fauriel, Saint-Etienne 42023, France

⁵Institut Carnot de Bourgogne, UMR CNRS 5209, 9 Avenue Alain Savary, BP 47870, 21078 Dijon cedex, France

Received

[*] Corresponding Author, philippe.lacorre@univ-lemans.fr

Abstract

The mixed ionic-electronic conductivity under dilute hydrogen, the stability and the catalytic activity under propane-air **type** mixtures of a series of LAMOX oxide-ion conductors have been studied. The effect of exposure to dilute hydrogen on the conductivity of the $\beta\text{-La}_2(\text{Mo}_{2-y}\text{W}_y)\text{O}_9$ series at 600°C depends on tungsten content: almost negligible for the highest ($y=1.4$), it is important for $\text{La}_2\text{Mo}_2\text{O}_9$ ($y=0$). In propane-air, all tested LAMOX electrolytes are stable at 600-700°C, but get reduced when water vapor is present. $\text{La}_2\text{Mo}_2\text{O}_9$ is the best oxidation catalyst of the series, with an activity comparable to that of nickel. The catalytic activity of other **tested** LAMOX compounds is much lower, $(\text{La}_{1.9}\text{Y}_{0.1})\text{Mo}_2\text{O}_9$ **showing** a deactivation phenomenon. These results suggest that, depending on composition, $\text{La}_2(\text{Mo}_{2-y}\text{W}_y)\text{O}_9$ compounds could be either electrolytes in single-chamber SOFC and dual-chamber micro-SOFC ($y=1.4$), or anode materials in dual-chamber SOFC (low y), or oxidation catalysts in SOFCs **operating with propane** ($y=0$).

Keywords: Oxidation Catalysis, LAMOX, Mixed Ionic Electronic Conduction, Propane, Reduction, Single or Dual Chamber, Solid Oxide Fuel Cell, Stability.

1 Introduction

The discovery, in $\text{La}_2\text{Mo}_2\text{O}_9$, of an oxide-ion conductivity higher than that of stabilized zirconias above 580°C [1] opened the prospect for using this material or its derivatives (the so-called LAMOX family [2]) as electrolyte in intermediate temperature solid oxide fuel cells (ITSOFCs). **Indeed**, it would lower the cell working temperature by about 150°C **in comparison** to standard 8mol%YSZ. However, the drawback of molybdates as electrolytes in conventional SOFC devices is **their tendency** to easily get reduced in hydrogen. It is for instance the case of Y substituted LAMOX which, when reduced, show additional electronic conductivity due to mixed-valent molybdenum [3]. However the reducibility of LAMOX compounds can be minimized through partial substitution **of molybdenum for tungsten** (up to ~75%) [4]. A careful examination of the stability phase diagram of W-substituted $\text{La}_2\text{Mo}_2\text{O}_9$ [5] shows that there is a region in $P(\text{O}_2)$ - T where $\text{La}_2\text{Mo}_2\text{O}_9$ can get reduced whereas $\text{La}_2(\text{Mo}_{0.5}\text{W}_{1.5})\text{O}_9$ remains stable. It opens up the way to **using** LAMOX compounds either as electrolyte or as anode materials, depending on SOFC configuration (conventional or single chamber) and on **operating** temperature. Moreover, both molybdenum and lanthanum are highly active catalytic elements in selective oxidation and oxidative dehydrogenation, and $\text{La}_2\text{Mo}_2\text{O}_9$ **has** already **been** known to be a catalyst for selective oxidation of toluene [6]. Therefore LAMOX materials might also be useful as oxidation catalysts for internal reforming at the anodic side of direct hydrocarbon SOFC devices [7].

The above considerations incited us to **undertake** a study on the electrical, catalytic and stability properties of a series of LAMOX compounds in hydrogen (ideal fuel for non polluting waste) and propane (ideal hydrocarbon for its high energy density in liquid form [8, 9]) fuel gas atmospheres. The aim was to test their ability to be used as multipurpose materials (electrolyte and/or anode and/or catalyst, depending on composition) in such devices as

single or dual chamber (be they hydrogen or direct hydrocarbon) intermediate temperature SOFCs. First results are presented here.

2 Experimental

2.1 Samples preparation

2.1.1 Powder samples

Reference and LAMOX powders used in this study were either commercial samples (Ni), or prepared by solid state reaction from commercial elementary oxides. Typical thermal treatments for the preparation of LAMOX compounds include a pre-annealing for 12h at 500°C (in order to avoid molybdenum oxide sublimation) followed by a series of annealings between 900 and 1225°C depending on composition, with intermediate grindings (heating/cooling rates of 5°C/min). At room temperature, all LAMOX compounds are obtained in their cubic β form, except for $\text{La}_2\text{Mo}_2\text{O}_9$ and $\text{Pr}_2\text{Mo}_2\text{O}_9$ which are in the monoclinic α form.

The $\text{La}_7\text{Mo}_7\text{O}_{30}$ sample used in the stability study under propane:air was prepared by partial reduction under dilute hydrogen of a $\text{La}_2\text{Mo}_2\text{O}_9$ powder sample (see [10]): a 1g sample of $\text{La}_2\text{Mo}_2\text{O}_9$ is annealed at 760°C under a 6vol% H_2 -94vol% N_2 flowing gas mixture until weight loss reaches about 1.117%, the theoretical value for $\text{La}_7\text{Mo}_7\text{O}_{30}$ **composition** (usually after 3-4h, a diffuse partial reduction plateau is reached). The heating and cooling rates in the same atmosphere were 30°C/min.

Phase purity was checked by X-ray diffraction, on a PANalytical θ/θ Bragg-Brentano X'pert MPD PRO diffractometer (CuK α_{1+2} radiations) equipped with an X'celerator detector (2θ range 5-130°, 2θ step 0.0084°, total counting time 5h).

2.1.2 Pellets

The $\text{La}_2(\text{Mo}_{2-y}\text{W}_y)\text{O}_9$ pellet samples used for the conductivity study were prepared from the previous powder batches with the same composition. Powders were first ball-milled in a FRITSCH planetary micromill pulverizette apparatus. The two agate vials containing ~900 mg of powder each, together with 6 agate balls (diameter ~1.2 cm) in ethanol, are rotated at 1120 rpm for four cycles of 15 min, with 15 min rest in between. Samples with about 300 mg of the previous ground powder, mixed with one drop of a solution of polyvinyl alcohol as an organic binder, were then shaped as pellets in a 5 mm diameter mould by uniaxial pressing at 500 MPa, followed by isostatic pressing at 500MPa. The **shaped** samples were heated at 400°C for 12h (heating rate 2°C/min) in order to decompose the organic binder, then sintered on Pt wedges for 3h at 1000°C for $y=0$, at 1175°C for $y=0.5$, or at 1225°C for $y=1$ and $y=1.4$ (heating rate 5°C/min). The relative densities were higher than 97(1)%.

2.2 Conductivity measurements

The total conductivity of the $\text{La}_2(\text{Mo}_{2-y}\text{W}_y)\text{O}_9$ pellet samples at different temperatures in air, in Ar and in commercial 90%Ar-10% H_2 mixture (Argon MHU10, Air Liquide) at total flowrate 0.6 L/h, was measured by complex impedance spectroscopy in the frequency range 13MHz-5Hz. For this purpose, a Hewlett Packard 4192 A frequency response analyzer was used. The measurements were performed at the open circuit voltage, and the applied AC voltage was 50 mV. Prior to measurements, thin film platinum electrodes (Pt paste) were deposited on both faces of each pellet sample. The samples were connected to the frequency response analyzer using platinum grids and wires, mounted in a stainless steel triple sample holder placed inside an alumina tube, and positioned in a Pyrox furnace. The properties of the three samples were therefore investigated almost simultaneously by semi-automatic measurement. The electrical properties of the pellet samples were measured in air while heating up, then in pure Argon at 608°C, then in the Ar- H_2 mixture for 24 h at the same temperature, and finally during cooling down from 608°C to RT in the Ar- H_2 atmosphere. The measurement is performed after at least 30 min of thermal stabilization.

The sample resistance was evaluated by intercepting data with the $\text{Re}(Z)$ axis. Occasionally, for the measurements in air, when this evaluation required the deconvolution of sample/electrode contribution, impedance data were fitted using a R//CPE electrical circuit with the equivalent circuit option of the ZVIEW program (Scribner Associates Inc.).

2.3 Measurements in propane-air atmospheres

Fuel:air mixtures are typical gas environment for single-chamber SOFC devices, which rely on the difference in catalytic activities between the anode and cathode materials (for hydrocarbon oxidation and oxygen reduction, respectively) [11, 12]. Due to the relatively large explosivity domain of these fuel mixtures, special care relative to gas balance should be taken for measurements in such atmospheres. Lower and Upper Explosivity Limits of propane volume percent in standard conditions (LEL=2.2vol% and UEL=10vol%, respectively [13]) enable two

possible working areas, which vary with temperature and pressure [13, 14] (see figure 1). High nitrogen inerting, which enables to prospect any $C_3H_8:O_2$ proportion, is recommended in order to avoid explosion risks.

2.3.1 Thermal stability

For stability tests of LAMOX compounds in propane:air mixture, we used a 16:84vol% propane:air proportion (above UEL), in propane excess relative to the optimal 10:90vol% propane:air proportion used in single-chamber SOFC [15, 16], in order to accelerate ageing while avoiding explosivity risks. In addition, the effect of nitrogen inerting (initial mixture diluted twice in nitrogen) and water vapor (around 2-3%, from gas bubbling in water) were measured.

For each composition, a single batch of around 500 mg of raw powder was placed in an alumina boat inside a tubular furnace allowing gas flowing, with variable area flowmeters controlling each gas flow. A thermal plateau with T equal to 600 or 700°C was applied for 24-72h in the gas mixture (with heating and cooling in nitrogen at 10°C/min).

After the thermal treatment, samples were characterized by X-ray diffraction (XRD). XRD patterns were recorded at room temperature on a Siemens D5000 diffractometer or on the PANalytical θ/θ Bragg-Brentano X'pert MPD PRO diffractometer (Cu $K\alpha_{1+2}$ radiations).

2.3.2 Catalytic activity

Catalytic tests were carried out below LEL in an oxygen-rich 1.8:98.2vol% propane:'air' gas mixture in order to avoid coking. Some tests were also performed in a 2:98vol% methane:'air' gas mixture. By 'air', we mean a 20:80vol% $O_2:He$ gas mixture.

Catalytic measurements were performed on a SWITCH 16 reactor System (AMTEC GmbH), which can contain up to 16 samples [17]. This system is built up from 16 tubular reactors (internal diameter 7 mm) placed in a heating device and individually connected to an inlet gas valve. All the tubing and valves are heated in order to avoid water vapor condensation. Feed and outflow gases are analyzed by gas chromatography (Agilent 3000 version QUAD instrument) equipped with Agilent 6890 thermal conductivity detectors (columns molecular sieve 5A, PoraPlot U and PoraPlot Q for O_2 , CH_4 , CO and CO_2 , C_3H_{8-x} , C_4H_{10-x} measurements), and Agilent 6850 flame ionization detectors (columns OV1 and Stabilwax for carboxylic acids and aldehydes measurements). The major part of water contained in the gas mixture is condensed upstream before the modules with a Peltier cooler. This device enables the study of a catalyst in a gas flow independently from the others, which are meanwhile submitted to an oxidizing atmosphere (20:80vol% $O_2:He$ gas mixture, with a 50 mL/min total flow for each sample). About 100 mg of each sample have been submitted to this oxidizing atmosphere at 400°C prior to catalytic measurements, which were performed under a 3 L/h total flow of 1.8vol% propane in the previous oxidizing atmosphere. Measurements were carried out as follows. The catalysts activity was measured in a sequential way, one after each other, at 400°C. Measurements were duplicated: the first one 2 minutes after the test starts (time t_2), and the second one 12 minutes later (time t_{14}). Meanwhile the other catalysts were exposed to 'air' flow. Thereby, all measurements were performed on « fresh / regenerated » catalysts, and problems due to activity measurements at different times could be avoided. After all reactors being studied, they were heated up under 'air' flow to the next temperature (450, 500, 550 and 600°C). A Ni sample and an empty reactor were used as reference catalyst and blank test, respectively.

3 Conductivity in dilute hydrogen

The total conductivity under dilute hydrogen of four samples of the $La_2(Mo_{2-y}W_y)O_9$ series ($y=0, 0.5, 1.0, 1.4$) was studied by impedance spectroscopy measurements. The first series of measurements were carried out at 608°C, first in air then in argon, and finally in a 10% H_2 -90%Ar mixture for 24h. In air and argon, the resistivity remained stable for all samples, and the measured values (R_0) were used as reference for further measurements in dilute hydrogen. Figure 2 shows the evolution with time of the relative resistivity R/R_0 for the four samples. The resistivity of the sample with highest W content ($y=1.4$) remains practically unchanged from Ar to $H_2:Ar$ mixture, whereas those of samples with lower W content decrease significantly in the first five hours. After about ten hours, the resistance seems to stabilize, suggesting that thermodynamic equilibrium could have been reached. The lowest the tungsten content is, the lowest the stabilized resistivity, therefore confirming that tungsten acts as a barrier against reduction, as previously evidenced [4]. Current measurements cannot differentiate between the ionic and electronic parts of conductivity. However the thermal evolution of total conductivity under dilute hydrogen, recorded while cooling down from 608°C, can give some hints about it (see figure 3a).

Figure 3 shows clearly that the total conductivity and activation energy measured on the oxidized phases while heating up in air, and on the reduced phases while cooling down in dilute hydrogen, are very different for the lowest W contents, where a huge increase in conductivity and a decrease in activation energy are observed. Here again, the lowest the W content, the more pronounced the effect (see figure 3b). These results are in agreement

with previous ones observed on Y/W doubly substituted LAMOX compounds [3]. Extra oxygen vacancies due to partial reduction could explain a slight increase in ionic mobility, but cannot justify alone a difference of several orders of magnitude in conductivity at low temperature. This, together with the lower activation energy, is more consistent with the appearance of electronic conductivity due to the occurrence of mixed valent molybdenum. In order to check the sample stability during the previous conductivity study in dilute hydrogen, we have performed room temperature X-ray diffraction measurements on the most sensitive pellet ($\text{La}_2\text{Mo}_2\text{O}_9$) before and after the conductivity measurements. Figure 4 shows that the LAMOX structure is kept during the thermal treatment at 608°C under dilute hydrogen, attesting that it can withstand partial reduction under these conditions without decomposing. However long term stability remains to be checked.

4 Stability and catalytic activity in propane-air

4.1 Stability

The main purpose of this stability study was to test whether LAMOX compounds of the tungsten series $\text{La}_2(\text{Mo}_{2-y}\text{W}_y)\text{O}_9$ can be stable as electrolytes in a single chamber SOFC propane:air atmosphere at working temperature (around 600-700°C), and whether reduced LAMOX compounds without tungsten can be stable as electrodes in the same conditions. The conditions for and main results of the study are reported in table 1.

The most reducible compound of the tungsten series, $y=0.25$, was not reduced in the propane:air mixture after 68h at 700°C. The powder remained white and the XRD pattern showed a cubic LAMOX type structure. Besides, condensation of a clear, water-like liquid was observed in the furnace tube and exit bubbler.

As stated in the experimental section, the effect of nitrogen inerting and water vapor (in order to mimic a fuel cell water production) were tested. When both elements are present in the gas mixture, their effect on the LAMOX phase stability is significant, specially at 700°C and whatever the W content ($y=0.25$ or 1.0): both samples become black and reduced to a major W-containing $\text{La}_7\text{Mo}_7\text{O}_{30}$ type phase [10] (from XRD). In addition to reduction, side effects are observed, such as coking (cold parts of furnace wall covered with soot), and condensation of a yellow viscous liquid. At 600°C, the same side effects are observed, but the $y=0.25$ powder remained white and LAMOX type from XRD. One can wonder whether reduction at 700°C is a direct effect of the gas mixture, or a side effect due to reaction with carbon after coking.

In order to check the importance of water in the above effects, a series of tests have been made with nitrogen inerting without water vapor (see table 1). At 600°C for 3 days, for all four sample tested, coking has disappeared. It seems therefore due to the presence of water. Correlatively, the powders remain LAMOX type, as controlled by XRD. One of the sample tested was $\text{La}_7\text{Mo}_7\text{O}_{30}$, a partially reduced form of $\text{La}_2\text{Mo}_2\text{O}_9$ with different structure [10], which appears to re-oxidise to $\text{La}_2\text{Mo}_2\text{O}_9$ in the dry inerted propane:air gas mixture.

4.2 Catalytic activity

As a preliminary remark, a few LAMOX compounds showed an initial peak of catalytic activity at time t_2 (2 min after start), followed by a decrease at time t_{14} (14 min after start). Such a transient phenomenon will be discussed below.

The catalytic activity for propane oxidation of the Ni and LAMOX compounds were recorded at different temperatures in stationary conditions at time t_{14} . The results are reported in figure 5. The blank test (with no sample) showed that no reaction takes place in the gas phase even at high temperature, thus discarding gas phase contribution. Not surprisingly, the Ni sample showed the highest catalytic activity at each temperature, with 98% of propane conversion at 600°C. $\text{La}_2\text{Mo}_2\text{O}_9$, both in its monoclinic ($T < 580^\circ\text{C}$) and in its cubic ($T > 580^\circ\text{C}$) crystalline forms [18], appears to be by far the most active of all LAMOX compounds at each temperature, with 79% of propane conversion at 600°C. All other tested substituted LAMOX compounds show a much lower activity (less than 15% at any temperature). In all cases, the almost exclusive formation of CO_2 and the presence of water traces not totally condensed in the Peltier cooler are characteristic of a full oxidation. When not lacking, only minimal traces of CO, C_3H_6 or derivatives could be identified (see table 2).

To illustrate the transient phenomenon mentioned above, the conversion rate of propane on $(\text{La}_{1.9}\text{Y}_{0.1})\text{Mo}_2\text{O}_9$ is shown on figure 6a. It is systematically higher than or equal to 20% at the initial measurement time t_2 , but drops dramatically at time t_{14} . Besides, the propane conversion rate at time t_2 is characterized by a carbon balance lower than 100%, which accounts for a carbon formation in the reactor (fig. 6b and table 2). At time t_{14} , the carbon balance catches up with 100%, but in this case the carbon retention effect is probably hidden by the low conversion rate of propane, as can be seen in table 2. Note however that, due to this low conversion rate of propane, the accuracy of selectivity measurements is probably rather lower here. After heating under 'air' flow, the sample activity is recovered. $\text{La}_2\text{Mo}_2\text{O}_9$ is also subject to deactivation at low temperature (fig. 6a), whereas it maintains its activity at higher temperature.

Other compounds, such as $\text{Pr}_2\text{Mo}_2\text{O}_9$ or $\text{La}_2(\text{Mo}_{1.9}\text{V}_{0.1})\text{O}_{8.95}$ exhibit a higher activity at time t_2 than at time t_{14} , which is accompanied with a carbon formation (data not shown). But in their cases, this phenomenon is observed

at one temperature only, which could suggest that their deactivation is irreversible. It is however difficult to draw firm conclusions from data that could correspond to measurement artifacts.

All LAMOX compounds tested in methane: 'air' atmosphere showed much lower activity than in propane: 'air' at the same temperatures. $\text{La}_2\text{Mo}_2\text{O}_9$ was still the most active catalyst, but with only 8% conversion rate of methane at 600°C. This result is in agreement with the usual observation that "methane is the most difficult hydrocarbon to oxidize, because CH_4 contains the strongest C–H bond of all alkanes" (see ^[19] and references therein).

5 Discussion and conclusion

The above study shows that LAMOX compounds, as a function of their composition, could be used as various components in a SOFC core depending on the cell configuration and operating temperature (see table 3). For dual-chamber configuration, conductivity measurements under dilute hydrogen on the $\text{La}_2(\text{Mo}_{2-y}\text{W}_y)\text{O}_9$ series suggest that the composition with highest tungsten content ($y=1.4$), provided that its electronic transport number is low enough (to be checked), could be used as electrolyte at intermediate temperature (below 600°C). It would necessitate a relatively thin electrolytic membrane (micro-SOFC geometry) in order to lower the ohmic losses. At the opposite, those LAMOX compounds with low tungsten content seem more suited as anode materials when H_2 is used as fuel, since their partial reduction make them mixed ionic-electronic conductors. More work is however needed to improve their electronic conductivity by finding the most appropriate compositions and reduction temperatures. In any case, the grain size and sample shaping are likely to affect the materials properties and thermal stability ^[20].

In single-chamber configuration, the tested LAMOX compounds appear to be stable as electrolyte (oxidized compounds) at 600-700°C in a characteristic dry propane:air mixture, inerted or not with nitrogen. It would preclude the use of reduced LAMOX compounds as anode materials in such environments, but we noticed that the presence of water in the gas mixture tends to favor LAMOX reduction. Since water vapor is not specially a reducing gas, a steam reforming (with gas shift) reaction probably takes place with propane and forms H_2 , which is a reducing agent. Since, in a SOFC device, water production is localised at the anodic side, further tests are needed in cell type configuration in order to determine whether the water production in the cell is able to stabilize or not a reduced LAMOX phase at the anode.

The exalted catalytic activity of $\text{La}_2\text{Mo}_2\text{O}_9$ for propane oxidation is clearly evidenced by this study. $\text{La}_2\text{Mo}_2\text{O}_9$ is the most active of tested LAMOX compounds, with a conversion rate almost equal to that of nickel. Additional experiments in a less oxidising propane:air mixture, or better in a direct propane SOFC, should be undertaken to characterize the selectivity of $\text{La}_2\text{Mo}_2\text{O}_9$ in order to evaluate the materials as anode in such devices. An alternative would be to design Ni- $\text{La}_2\text{Mo}_2\text{O}_9$ cermet since $\text{La}_2\text{Mo}_2\text{O}_9$ is unreactive with nickel ^[21].

The impact of substitution on the LAMOX catalytic activities are still unclear and should be subject to further investigations. However, we can give some assumptions. Like VI-B transition metal, Mo oxides and mixed oxides are well known for their capacities for hydrocarbon activation ^[22]. Thus we can anticipate that chemical substitutions could lead, depending on their nature, to more or less surface depreciation of Mo content, thus reducing or even preventing the catalytic activity. However, a strong interaction with some substituting elements, which may reduce the acid feature of Mo oxides, can not be ruled out. Whatever its form, the carbon formation observed in LAMOX compounds such as $(\text{La}_{1.9}\text{Y}_{0.1})\text{Mo}_2\text{O}_9$, concomitantly with their deactivation, is also likely to block the access to active sites. Complementary studies are necessary to elucidate these phenomena.

Finally the results presented in this paper suggest that LAMOX materials, due to their versatility (see table 3), might be suited to specific SOFC designs with composition gradients, which would minimize reactivity between the cell components and therefore ageing problems.

Acknowledgements

The authors thank Arnold Desmartin-Chomel (IRCELYON) for his help with catalytic measurements. ADEME (the French Agency for Environment and Energy Mastering) and Région Pays de la Loire are acknowledged for J. Jacquens PhD thesis grant, as well as ECOS-SUD program for its support to this work (project A07E03). The authors deplore the lack of any support by French ANR (Research National Agency) despite several proposals. This paper was presented at the Fundamental and Developments of Fuel Cells 2008 Conference (FDFC08) held in Nancy, France, on Dec. 10-12th, 2008.

References

- 1
2
3
4
5
6
7
8
9
10
11
12
13
14
15
16
17
18
19
20
21
22
23
24
25
26
27
28
29
30
31
32
33
34
35
36
37
38
39
40
41
42
43
44
45
46
47
48
49
50
51
52
53
54
55
56
57
58
59
60
- [1] P. Lacorre, F. Goutenoire, O. Bohnke, R. Retoux, Y. Laligant, *Nature* **2000**, *404*, 856.
[2] F. Goutenoire, O. Isnard, E. Suard, O. Bohnke, Y. Laligant, R. Retoux, P. Lacorre, *Journal of Materials Chemistry* **2001**, *11*, 119.
[3] P. Pinet, J. Fouletier, S. Georges, *Materials Research Bulletin* **2007**, *42*, 935.
[4] S. Georges, F. Goutenoire, Y. Laligant, P. Lacorre, *Journal of Materials Chemistry* **2003**, *13*, 2317.
[5] D. Marrero-Lopez, J. Canales-Vazquez, J. C. Ruiz-Morales, J. T. S. Irvine, R. Nunez, *Electrochimica Acta* **2005**, *50*, 4385.
[6] W. X. Kuang, Y. N. Fan, J. H. Qiu, Y. Chen, *Journal of Materials Chemistry* **1998**, *8*, 19.
[7] S. McIntosh, R. J. Gorte, *Chemical Reviews* **2004**, *104*, 4845.
[8] Z. L. Zhan, J. Liu, S. A. Barnett, *Applied Catalysis a-General* **2004**, *262*, 255.
[9] P. K. Cheekatamarla, C. M. Finnerty, J. Cai, *International Journal of Hydrogen Energy* **2008**, *33*, 1853.
[10] F. Goutenoire, R. Retoux, E. Suard, P. Lacorre, *Journal of Solid State Chemistry* **1999**, *142*, 228.
[11] T. Hibino, A. Hashimoto, T. Inoue, J. Tokuno, S. Yoshida, M. Sano, *Science* **2000**, *288*, 2031.
[12] Z. P. Shao, S. M. Haile, J. Ahn, P. D. Ronney, Z. L. Zhan, S. A. Barnett, *Nature* **2005**, *435*, 795.
[13] J. M. Petit, J. L. Poyard, *Rapport INRS* **2004**, *Brochure ED 911*.
[14] A. Bentaib, J. Vendel, *Rapport Scientifique et Technique IRSN* **2006**, *Recherche sur les accidents*.
[15] I. C. Stefan, C. P. Jacobson, S. J. Visco, L. C. De Jonghe, *Electrochemical and Solid State Letters* **2004**, *7*, A198.
[16] M. Yano, A. Tomita, M. Sano, T. Hibino, *Solid State Ionics* **2007**, *177*, 3351.
[17] G. Morra, A. Desmartin-Chomel, C. Daniel, U. Ravon, D. Farrusseng, R. Cowan, A. Krusche, C. Mirodatos, *Chemical Engineering Journal* **2008**, *138*, 379.
[18] F. Goutenoire, O. Isnard, R. Retoux, P. Lacorre, *Chemistry of Materials* **2000**, *12*, 2575.
[19] O. Demoulin, B. Le Clef, M. Navez, P. Ruiz, *Applied Catalysis A-General* **2008**, *344*, 1.
[20] A. Selmi, G. Corbel, S. Kojikian, V. Voronkova, E. Kharitonova, P. Lacorre, *European Journal of Inorganic Chemistry* **2008**, 1813.
[21] G. Corbel, P. Lacorre, *Journal of Solid State Chemistry* **2006**, *179*, 1339.
[22] V. D. Sokolovskii, *Catalysis Reviews-Science and Engineering* **1990**, *32*, 1.

Tables

Table 1. Conditions for the stability measurements of LAMOX powders in propane-air mixtures and final products.

Initial compounds	Gas mixture	Flow (L/h)	T(°C)	t(h)	Products
$\text{La}_2(\text{Mo}_{1.75}\text{W}_{0.25})\text{O}_9$	C_3H_8 :air	0.8:4.2	700	24	white LAMOX
$\text{La}_2(\text{Mo}_{1.75}\text{W}_{0.25})\text{O}_9$	"	"	"	68	white LAMOX
$\text{La}_2(\text{Mo}_{1.75}\text{W}_{0.25})\text{O}_9$	C_3H_8 :air: N_2 + H_2O	0.8:4.2:5+bubbles	700	42	black $\text{La}_7\text{Mo}_7\text{O}_{30}$ type
$\text{La}_2(\text{MoW})\text{O}_9$	"	"	"	72	black $\text{La}_7\text{Mo}_7\text{O}_{30}$ type
$\text{La}_2(\text{Mo}_{1.75}\text{W}_{0.25})\text{O}_9$	"	"	600	42	white LAMOX
$\text{La}_2\text{Mo}_2\text{O}_9$	C_3H_8 :air: N_2	0.8:4.2:5	600	72	white $\text{La}_2\text{Mo}_2\text{O}_9$
$\text{La}_7\text{Mo}_7\text{O}_{30}$	"	"	"	"	white $\text{La}_2\text{Mo}_2\text{O}_9$
$\text{La}_2(\text{Mo}_{1.9}\text{V}_{0.1})\text{O}_{8.95}$	"	"	"	"	grey LAMOX
$\text{La}_2(\text{Mo}_{1.75}\text{W}_{0.25})\text{O}_9$	"	"	"	"	grey LAMOX

Table 2. Catalytic performances of Ni, La₂Mo₂O₉ and La_{1.9}Y_{0.1}Mo₂O₉ in 1.8:98.2vol% propane:‘air’ mixture at different temperatures and reaction advancement (selectivity of gas products as measured by gas chromatography, and undetected C as deduced from carbon balance in the gas phase)^a

Compound	T (°C)	conversion O ₂ (%)		conversion C ₃ H ₈ (%)		C selectivity (%) ^b							
						CO ₂		CO		C ₃ H ₆		undetected C	
		2'	14'	2'	14'	2'	14'	2'	14'	2'	14'	2'	14'
Ni	400	19	20	18	19	71	73	0	0	4	4	25	23
	450	28	29	43	46	88	88	0	0	4	3	8	9
	500	38	38	73	75	95	94	0	0	2	2	3	4
	550	45	44	92	93	98	96	0	0	1	1	1	3
	600	45	46	99	98	87	98	0	0	0	0	13	2
La ₂ Mo ₂ O ₉	400	15	14	19	12	54	95	0	0	0	1	46	4
	450	21	21	30	26	86	99	0	0	1	1	13	0
	500	27	27	49	47	93	99	0	0	1	1	6	0
	550	32	32	64	62	95	99	0	0	1	1	4	0
	600	37	37	80	78	96	99	0	0	1	1	3	0
La _{1.9} Y _{0.1} Mo ₂ O ₉	400	13	13	18	3	6	38	0	0	0	0	94	62
	450	14	14	19	4	11	61	0	0	0	0	89	39
	500	15	15	21	7	19	77	0	0	0	1	81	22
	550	16	16	25	9	24	82	0	0	1	4	75	14
	600	16	15	28	11	24	57	0	1	3	11	73	31

^a Other gas tested, either measured as traces or not detected: CH₄, i-C₄H₁₀, i-C₄H₈, C₂H₄O (acetaldehyde), C₃H₄O (acrolein), C₃H₆O (acetone and propionaldehyde and allyl alcohol), C₂H₄O₂ (acetic acid), C₃H₆O₂ (propionic acid), C₃H₄O₂ (acrylic acid).

^b C selectivity was calculated as the number of carbon atom moles in the given product divided by 3 times the number of moles of propane reacted.

Table 3. Overview of possible use of LAMOX compounds in SOFC devices, as deduced from the current study.

SOFC	Dual chamber	Single chamber
Electrolyte	Micro-SOFC: high W content, low T (500°C) Macro-SOFC: protective layer necessary	Electrolyte stable in dry propane:air atmosphere
Anode	Low W content (composition to be optimized as a function of operating temperature)	Reduction favored by water produced at anode ?
Anodic catalyst	La ₂ Mo ₂ O ₉ good oxidation catalyst of propane (to be tested in direct hydrocarbon SOFC)	La ₂ Mo ₂ O ₉ good oxidation catalyst of propane (to be tested in SCFC)

Figure caption

Fig. 1 : Schematic extrapolation of the Shapiro diagram for $C_3H_8-O_2-N_2$.

Fig. 2 : Time dependence of $La_2(Mo_{2-y}W_y)O_9$ relative resistivity at 608°C under dilute hydrogen.

Fig. 3 : a) Conductivity curves of $La_2(Mo_{2-y}W_y)O_9$ in air (heating up) and in diluted hydrogen (cooling down).
b) Total conductivity, at 300°C and 600°C in air and in diluted hydrogen, as a function of tungsten amount. In first approximation, grey areas are assumed to roughly represent electronic contributions.

Fig. 4 : Room temperature X-ray diffraction patterns of the $La_2Mo_2O_9$ pellet before and after the conductivity measurements under dilute hydrogen (after polishing the Pt electrode layer).

Fig. 5 : Conversion rates of propane (full oxidation) at different temperatures on a series of LAMOX oxide-ion conductors, compared to that of nickel (measurements performed in stationary conditions after 14 min of propane: 'air' exposure).

Codes for composition : Ax-LM = $La_{2-x}A_xMo_2O_{9-\delta}$, LM-By = $La_2Mo_{2-y}B_yO_{9-\delta}$.

Fig. 6 : Propane conversion rate (a) and carbon balance (b) during the catalytic activity measurements of $La_2Mo_2O_9$ and $(La_{1.9}Y_{0.1})Mo_2O_9$. Carbon balance corresponds to the ratio between carbon amount detected in the outflow gas mixture and carbon amount in the feeding gas mixture.

Grey areas represent 'air' feeding periods, measurements being made in propane: 'air' mixture at time t_2 and t_{14} .

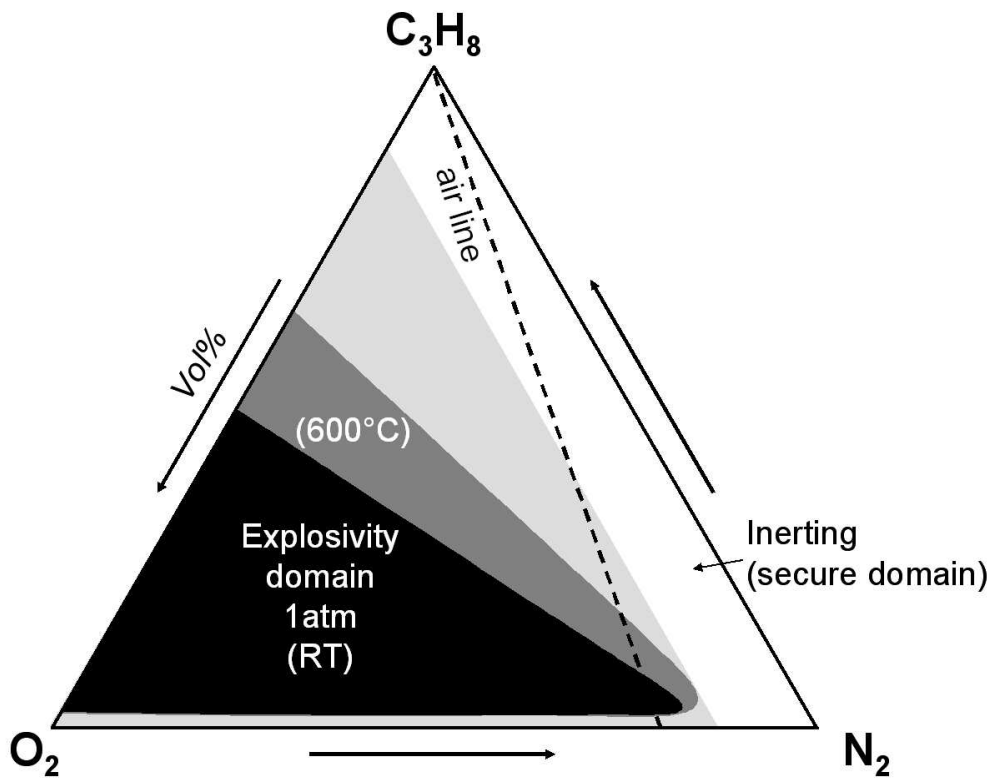


Fig. 1 : Schematic extrapolation of the Shapiro diagram for C₃H₈-O₂-N₂.
50x39mm (600 x 600 DPI)

review

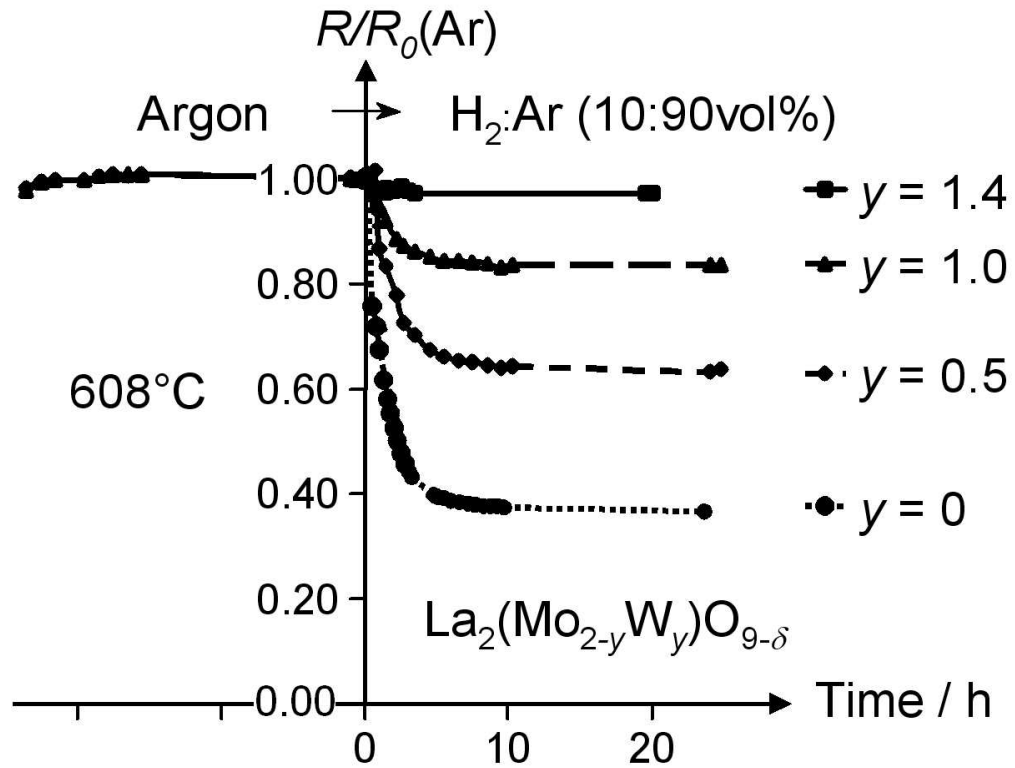


Fig. 2 : Time dependence of $\text{La}_2(\text{Mo}_{2-y}\text{W}_y)\text{O}_9$ relative resistivity at 608°C under dilute hydrogen.
50x39mm (600 x 600 DPI)

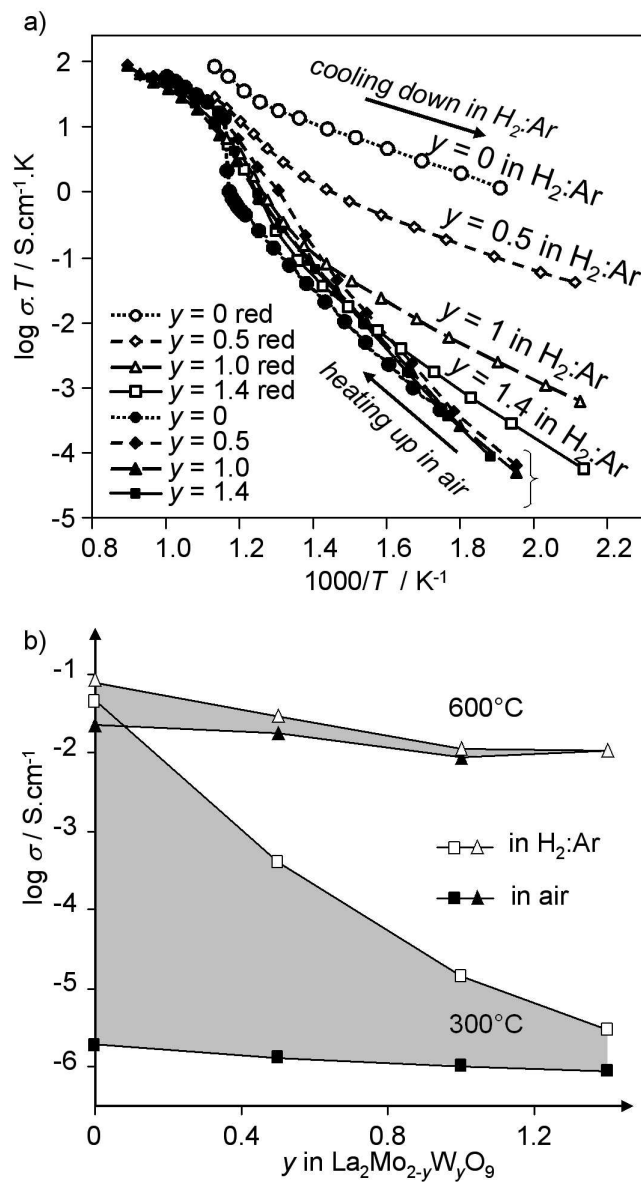


Fig. 3 : a) Conductivity curves of $\text{La}_2(\text{Mo}_{2-y}\text{W}_y)\text{O}_9$ in air (heating up) and in diluted hydrogen (cooling down).
 b) Total conductivity, at 300°C and 600°C in air and in diluted hydrogen, as a function of tungsten amount. In first approximation, grey areas are assumed to roughly represent electronic contributions.
 46x84mm (600 x 600 DPI)

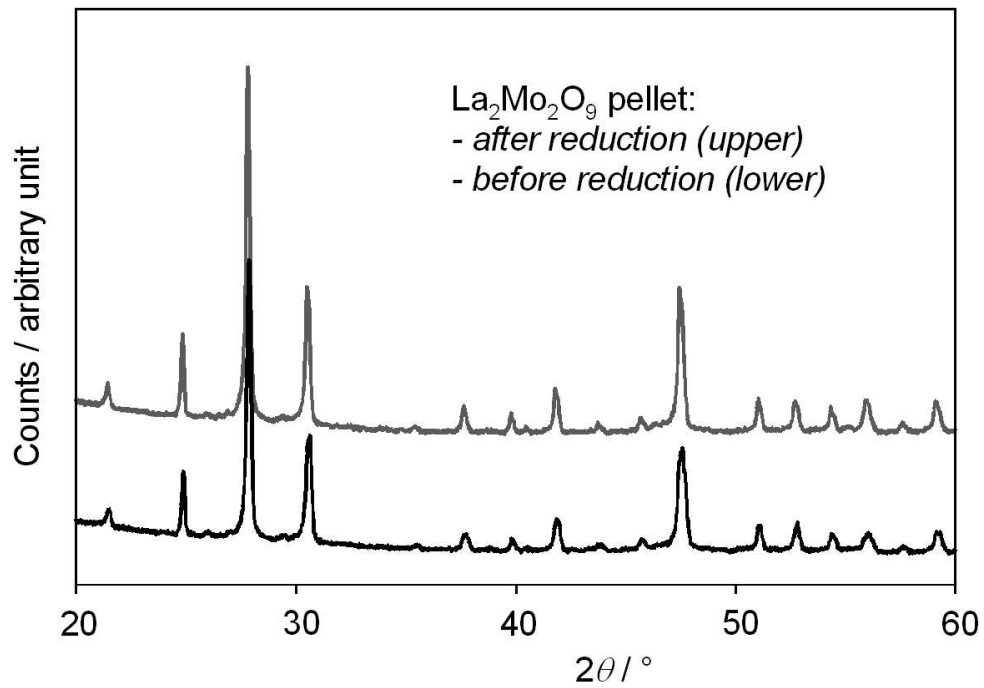


Fig. 4 : Room temperature X-ray diffraction patterns of the $\text{La}_2\text{Mo}_2\text{O}_9$ pellet before and after the conductivity measurements under dilute hydrogen (after polishing the Pt electrode layer).
50x35mm (600 x 600 DPI)

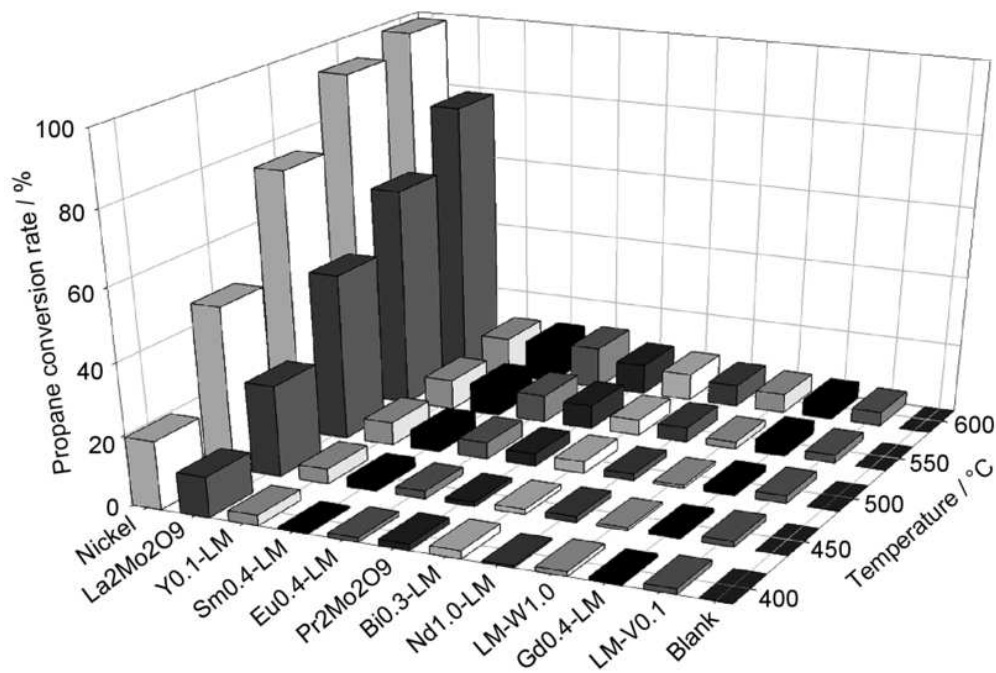


Fig. 5 : Conversion rates of propane (full oxidation) at different temperatures on a series of LAMOX oxide-ion conductors, compared to that of nickel (measurements performed in stationary conditions after 14 min of propane:'air' exposure).

Codes for composition : Ax-LM = $\text{La}_{2-x}\text{AxMo}_2\text{O}_9-\delta$, LM-By = $\text{La}_2\text{Mo}_{2-y}\text{ByO}_9-\delta$.
34x23mm (600 x 600 DPI)

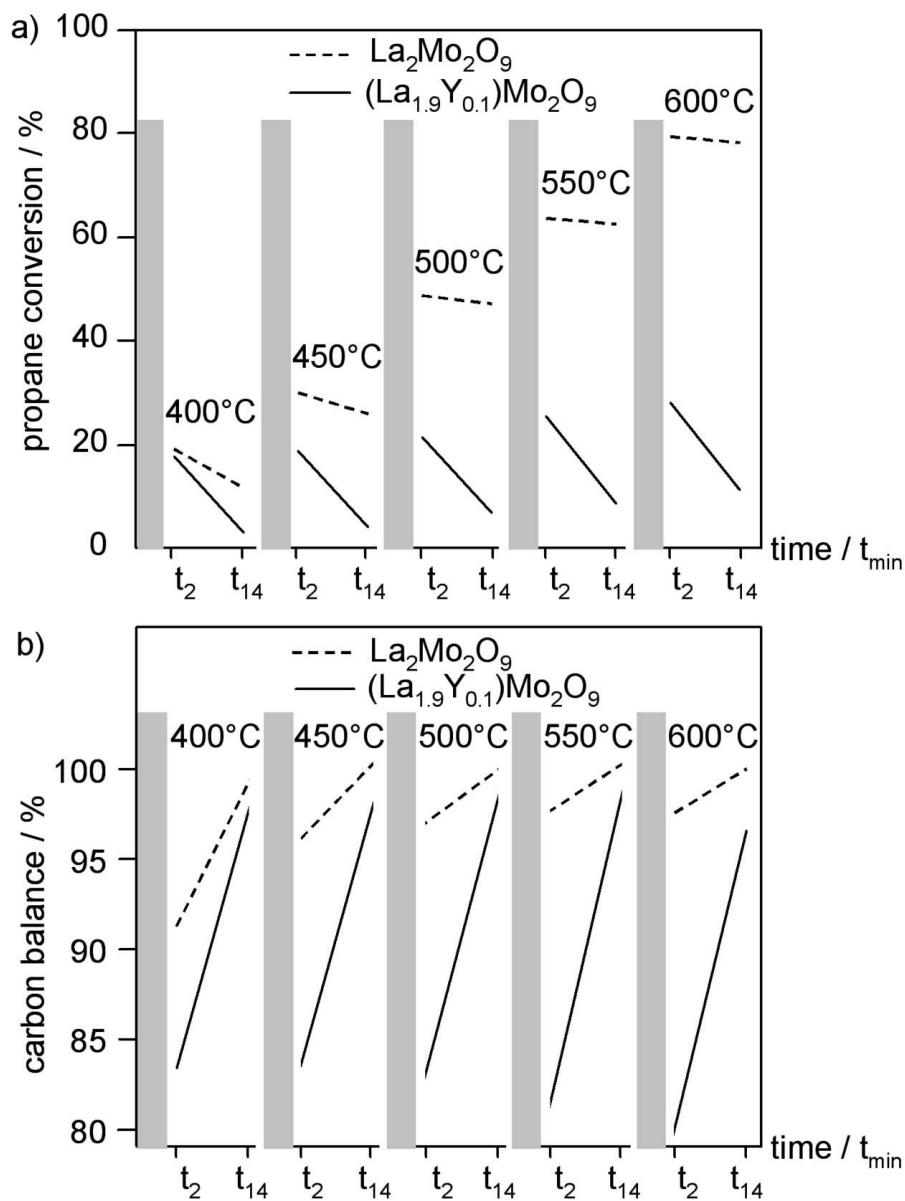


Fig. 6 :Propane conversion rate (a) and carbon balance (b) during the catalytic activity measurements of $\text{La}_2\text{Mo}_2\text{O}_9$ and $(\text{La}_{1.9}\text{Y}_{0.1})\text{Mo}_2\text{O}_9$. Carbon balance corresponds to the ratio between carbon amount detected in the outflow gas mixture and carbon amount in the feeding gas mixture.

Grey areas represent 'air' feeding periods, measurements being made in propane:'air' mixture at time t_2 and t_{14} .

54x70mm (600 x 600 DPI)